OXFORD

Carcinogenesis, 2020, Vol. 41, No. 11, 1518–1528

doi:10.1093/carcin/bgaa059
Advance Access publication June 30, 2020
Original Article

ORIGINAL ARTICLE

Modulation of the PD-1/PD-L1 immune checkpoint axis during inflammation-associated lung tumorigenesis

Sreekanth Chanickal Narayanapillai[1], Yong Hwan Han[1], Jung Min Song[1], Manaye Ebabu Kebede[1], Pramod Upadhyaya[1] and Fekadu Kassie[1,2,*]

[1]Masonic Cancer Center, University of Minnesota, Minneapolis, MN 55455, USA and [2]College of Veterinary Medicine, University of Minnesota, Saint Paul, MN 55108, USA

*To whom correspondence should be addressed. Tel: +1 612 625 9637; Fax: +1 612 626 5135; Email: kassi012@umn.edu

Abstract

Chronic obstructive pulmonary disease (COPD) is a significant risk factor for lung cancer. One potential mechanism through which COPD contributes to lung cancer development could be through generation of an immunosuppressive microenvironment that allows tumor formation and progression. In this study, we compared the status of immune cells and immune checkpoint proteins in lung tumors induced by the tobacco smoke carcinogen 4-(methylnitrosamino)-1-(3-pyridyl)-1-butanone (NNK) or NNK + lipopolysaccharide (LPS), a model for COPD-associated lung tumors. Compared with NNK-induced lung tumors, NNK+LPS-induced lung tumors exhibited an immunosuppressive microenvironment characterized by higher relative abundances of PD-1$^+$ tumor-associated macrophages, PD-L1$^+$ tumor cells, PD-1$^+$ CD4 and CD8 T lymphocytes and FOXP3$^+$ CD4 and CD8 T lymphocytes. Also, these markers were more abundant in the tumor tissue than in the surrounding 'normal' lung tissue of NNK+LPS-induced lung tumors. PD-L1 expression in lung tumors was associated with IFNγ/STAT1/STAT3 signaling axis. In cell line models, PD-L1 expression was found to be significantly enhanced in phorbol-12-myristate 13-acetate activated THP-1 human monocytes (macrophages) treated with LPS or incubated in conditioned media (CM) generated by non-small cell lung cancer (NSCLC) cells. Similarly, when NSCLC cells were incubated in CM generated by activated THP-1 cells, PD-L1 expression was upregulated in EGFR- and ERK-dependent manner. Overall, our observations indicate that COPD-like chronic inflammation creates a favorable immunosuppressive microenvironment for tumor development and COPD-associated lung tumors might show a better response to immune checkpoint therapies.

Introduction

Lung cancer is the leading cause of cancer-related mortality in the USA (1). According to the American Cancer Society, in 2019, ~228 150 new cases of lung cancer would be diagnosed and there would be 142 670 lung cancer-related deaths, accounting for ~26% of all cancer deaths. Although tobacco smoke carcinogens stand as the main etiologic factor of lung cancer, several factors increase susceptibility to this malignancy. In particular, in patients with moderate-to-severe chronic obstructive pulmonary disease (COPD), the prevalence of lung cancer can go up as high as 5-fold that of smokers without the disease (2–4). Biological mechanisms that may predispose COPD patients to a higher incidence of lung cancer include oxidative stress and the resulting DNA damage and gene mutation, chronic exposure to proinflammatory cytokines and chemokines, repression of DNA repair and increased cell proliferation and survival (5–7). Also, emerging data suggest that the expression of immune checkpoint proteins programmed cell death 1 (PD-1) and programmed cell death 1 ligand 1 (PD-L1) is dysregulated in COPD patients (8–10). However, the role of the PD-1/PD-L1 axis in the context of COPD-associated lung tumorigenesis is unclear.

PD-1 is a transmembrane protein expressed on the surface of immune cells (11), whereas its ligand PD-L1 is expressed on tumor cells as well as immune cells (12–14). PD-L1 expression is prevalent in non-small cell lung cancer (NSCLC) (15), and the

Received: July 31, 2019; **Revised:** May 28, 2020;

Abbreviations

COPD	chronic obstructive pulmonary disease
CM	conditioned media
EGFR	epidermal growth factor receptor
ERK	extracellular signal-regulated kinase
IL	interleukin
LPS	lipopolysaccharide
NNK	4-(methylnitrosamino)-1-(3-pyridyl)-1-butanone
NSCLC	non-small cell lung cancer
NTHi	Haemophilus infuenzae
PD-1	programmed cell death 1
PD-L1	programmed cell death 1 ligand 1
PMA	phorbol-12-myristate 13-acetate
SNLT	surrounding 'normal' lung tissue
TAM	tumor-associated macrophages
TANs	tumor-associated neutrophils

interaction between PD-L1 and PD-1 result in the suppression of cytotoxic $CD8^+$ T lymphocyte recruitment, survival and function, and ultimately the loss of an effective anti-tumor immune response (15–18). Recent revolutionary lung cancer therapeutic strategies using anti-PD-L1 and anti-PD-1 monoclonal antibodies have been shown to restore T cell–mediated anti-tumor immunity and provide durable remissions (19–22). However, the overall response rate of patients was only ~15% (19,22), indicating the need to identify biomarkers of response to immune checkpoint blockade. In this regard, some recent reports have shown that lung cancer patients with COPD exhibited a higher response to PD-1 blockade compared with lung cancer patients without COPD (9,23,24). However, the role of chronic inflammation in tipping the balance of immune cells and immune checkpoint proteins to promote lung tumors and thereby enhance the response to immune checkpoint blockade is unclear.

In the present study, we compared the status of immune cells and immune checkpoint proteins in lung tumors induced by 4-(methylnitrosamino)-1-(3-pyridyl)-1-butanone (NNK) or NNK + lipopolysaccharide (LPS), a model for COPD-associated lung tumors (25). We observed that NNK+LPS-induced lung tumors differentially exhibited an immunosuppressive microenvironment characterized by higher abundance of tumor-associated macrophages (TAMs), TAMs with M2 phenotype, $PD\text{-}1^+$ TAMs, $PD\text{-}L1^+$ tumor cells, $PD\text{-}1^+$ CD4 and CD8 T lymphocytes and $FOXP3^+$ CD4 and CD8 T lymphocytes compared with the level in NNK-induced lung tumors. The abundance of these markers was also higher in the tumor tissue than in the surrounding 'normal' lung tissue (SNLT) of NNK+LPS-induced lung tumors. Moreover, under *in vitro* conditions, incubation of phorbol-12-myristate 13-acetate activated THP-1 human monocytes (macrophages) with LPS or condition media (CM) generated by NSCLC cells enhanced PD-L1 expression. Similar findings were observed upon incubation of NSCLC cells in CM generated by activated THP-1 cells and, in epidermal growth factor receptor (EGFR) mutant H1975 NSCLC cells, these effects appear to be mediated via EGFR and extracellular signal-regulated kinase (ERK) signaling pathways as specific inhibitors of EGFR and ERK activation suppressed PD-L1 levels. Overall, our observations indicate that COPD-like chronic inflammation creates a favorable immunosuppressive microenvironment for tumor development and progression and the overexpression of PD-L1 and PD-1 in COPD-associated lung tumors may lead to a better response to immune checkpoint blockade.

Materials and methods

Cells and reagents

The NSCLC cell line A549 was obtained from Caliper Life Sciences (Waltham, MA). H838 cells were kindly obtained from Dr Robert Kratzke (University of Minnesota). H1650 and H1975 cell lines were obtained from Dr Shujun Liu (Hormel Institute, MN). Human THP-1 monocytes were kindly provided by Dr Schwertfeger (Twin Cities, MN). The cell lines have been regularly tested for mycoplasma infection and the authenticity of the cells was determined by short tandem repeat analysis technology at MD Anderson`s Cell Line Core Facility. All cell lines were cultured in RPMI-1640 media (Thermo Fisher Scientific, Waltham, MA) supplemented with 10% fetal bovine serum (Thermo Fisher Scientific) in 5% CO_2 incubator at 37°C. All antibodies for Western immunoblotting studies were purchased from Cell Signaling Technology (Beverly, MA). Specific siRNAs against human *COX-2* gene (cat. no. GS5743), STAT1 (cat. no. GS6772) and non-silencing AllStars Negative Control siRNA (cat. no. SI03650318) were purchased from Qiagen (Germantown, MD). All other reagents were purchased from Sigma–Aldrich (St Louis, MO) unless otherwise specified.

Lung tumor bioassay in mice

Six-week-old female A/J mice were obtained from the Jackson Laboratory (Bar Harbor, ME) and housed in the specific-pathogen-free animal quarters of Research Animal Resources, University of Minnesota Academic Health Center. After 1 week of acclimatization, mice were randomized into three treatment groups (20 mice per group). Mice in normal control group (group 1) received physiological saline solution, the vehicle control. Mice in groups 2 and 3 were treated with two doses of NNK (100 mg/kg, i.p.) at an interval of a week. Beginning 1 week after the second NNK dose, mice in group 3 received weekly intranasal instillations of the proinflammatory endotoxin LPS (5 μg/mouse in 50 μl of physiological saline solution) for 14 weeks. At week 30, mice were euthanized with an overdose of CO_2, lungs harvested and tumors on the surface of the lung counted. Subsequently, lung tumors were dissected and used, together with the surrounding 'normal' lung tissue (SNLT), for downstream flow cytometry-based analysis.

Tissue processing

Lung tumors or SNLT from NNK- or NNK+LPS-treated mice or normal lung tissues from the vehicle-treated mice were mechanically dissociated and digested with Collagenase/Dispase (1 mg/ml; Roche) and DNase I (0.15 mg/ml; Sigma–Aldrich) in phosphate-buffered saline for 1 h at 37°C water bath under agitation every 8–10 min. Upon completion of tissue digestion, 30 ml of 2% bovine serum albumin in phosphate-buffered saline was added and the resulting cell suspensions were strained through a 100 μm cell strainer to remove the non-digested tissue. Red blood cells were removed by a solution containing NH_4Cl (0.15 M), $KHCO_3$ (10 mM) and Na_2EDTA (100 mM, pH 7.2).

Flow cytometry

After cells were counted, 1 million cells per sample were re-suspended in 100 μl of staining buffer (phosphate-buffered saline plus 2% fetal bovine serum) and incubated with Mouse BD Fc Block (anti-mouse CD16/CD32; BD Pharmingen) on ice for a minimum 30 min. Cells were subsequently stained for 30 min on ice with antibodies for cell surface markers (list of antibodies are included as Supplementary Table 3, available at *Carcinogenesis* Online). For FOXP3 intracellular staining, cells were permeabilized with the Mouse FOXP3 Buffer Set (BD Pharmingen) according to the manufacturer's instructions and incubated in the dark at room temperature for 30 min with anti-mouse FOXP3-PE-Cy5 (BD Biosciences). Data were acquired with a BD LSRII flow cytometer using BD FACSDiva software (BD Bioscience) and analyzed using Flowjo v10 (Flowjo, LLC). The gating strategy and markers for different cell types are listed as Supplementary Table 1 (available at *Carcinogenesis* Online).

Incubation of THP-1 cells in conditioned media prepared from NSCLC cells

To assess whether conditioned media (CM) from NSCLC cells induce PD-1 and/or PD-L1 in THP-1 cells, NSCLC cells were grown in complete RPMI

1640 media for 48 h, washed three times with serum-free media and then further grown in serum-free media for 24 h. Subsequently, the CM were collected, centrifuged at 15 000 rpm for 15 min to remove non-adherent cells and debris, and the supernatants collected were used to grow the human monocytic THP-1 cells activated with phorbol 12-myristate 13-acetate (PMA, 100 ng/mL).

Incubation of NSCLC cells in CM generated by activated THP-1 cells

To examine whether CM from activated human monocyte THP-1 cells induces the immune checkpoint molecule PD-L1 in NSCLC cells, THP-1 cells were cultured in serum-free RPMI-1640 media containing PMA for 48 h. Subsequently, the CM were collected, centrifuged at 15 000 rpm for 15 min to remove non-adherent cells and debris and the supernatants collected and used to grow NSCLC cells.

Transfection of siRNA

Activated THP-1 macrophages were transfected with specific siRNAs against *COX-2* gene or negative control siRNA using HiPerFect transection reagent following manufacturer's instructions (Qiagen). Briefly, THP-1 monocytes were differentiated into macrophages using 100 ng/ml PMA treatment for 48 h and transfected with 50 nM each of the four Cox-2 siRNAs or negative control siRNA following the manufacturer's instructions (Qiagen). Post-transfection, THP-1 macrophages were grown under normal conditions for 24 h and used for further experiments.

Western immunoblot assay

For Western immunoblot analysis, cells were suspended in RIPA buffer containing protease and phosphatase inhibitors on ice for 20 min followed by centrifugation for 20 min at 13 500 rpm, 4°C. The protein concentration of the supernatants was determined using the Pierce BCA protein Assay kit (Thermo Fisher Scientific). Total cell proteins were subjected to electrophoresis on 4–12% gradient sodium dodecyl sulfate gels, and the proteins were transferred onto polyvinylidene difluoride membranes (Bio-Rad, Hercules, CA). The membranes were probed with either anti-EGFR, anti-STAT3, anti-STAT1, anti-ERK, anti-Akt, anti-PD-L1, anti-COX-2, anti-β-actin or anti-GAPDH, followed by a secondary antibody conjugated to horseradish peroxidase. All immunoblots were visualized by SuperSignal West Pico Chemiluminescent Substrate (Thermo Fisher Scientific).

Quantitative reverse transcription–PCR analysis

Total RNA was extracted using the miRNeasy Mini Kit (Qiagen, Valencia, CA) according to the manufacturer's instruction. The purity and integrity of total RNA were confirmed by Nanodrop. The first-strand complementary DNA was synthesized, and quantitative reverse transcription–PCR performed following standard procedures using gene-specific forward and reverse primers. The primer sequences for the different genes are listed as Supplementary Table 2 (available at *Carcinogenesis* Online). All samples were normalized to an internal control gene, *ACTB* and the comparative Ct method was used to assess the relative gene expression. Samples were tested in triplicates and repeated three times.

Statistical analysis

Significant differences between groups were determined using Student's unpaired *t*-test and one-way analysis of variance. All analyses were performed using GraphPad Prism, version 5.0 (GraphPad Software, San Diego, CA). Data are shown as means ± SEMs. $P < 0.05$ was considered statistically significant.

Results

COPD-like chronic inflammation induced by LPS increased the multiplicity and size of NNK-induced lung tumors

Our previous studies (25) showed that the multiplicity of lung tumors in mice treated with LPS alone was in the range of spontaneous tumor rate (0–1 tumor per mouse). Therefore, in the present study, LPS group was not included. Treatment of A/J mice with NNK alone induced 14 ± 4 tumors per mouse, whereas chronic administration of LPS to NNK pretreated mice significantly increased the lung tumor multiplicity by more than 2-fold to 33 ± 10 lung tumors per mouse ($P < 0.05$, Supplementary Figure 1A, available at *Carcinogenesis* Online). Classification of the lung tumors based on their diameter indicated that most of the lung tumors in the NNK group were small (<1 mm) and larger tumors (>2 mm) were absent, whereas 7 ± 3 and 13 ± 4 lung tumors per mouse in the NNK + LPS group had a size of >2 and 1–2 mm, respectively, indicating that LPS treatment increased not only lung tumor multiplicity but also lung tumor size (Supplementary Figure 1B, available at *Carcinogenesis* Online).

Abundance of TAMs and tumor-associated neutrophils in NNK- and NNK+LPS-induced lung tumors

To compare the relative recruitment of TAMs and tumor-associated neutrophils (TANs) to NNK- and NNK+LPS-induced lung tumors, the abundance of $CD45^+$ $CD11c^+$ $CD11b^-$ and $CD45^+$ $CD11c^-$ $CD11b^+$ cells, which represent TAMs and TANs, respectively, was determined by flow cytometry. Figure 1A and B show representative flow cytometry plots for TAMs ($CD45^+CD11c^+CD11b^-$) and TANs ($CD45^+CD11b^+Ly6G^+$), whereas Figure 1A-i and B-i depicts quantification of TAMs and TANs, respectively. The abundance of TAMs was more than 2-fold higher in NNK+LPS-induced tumors compared with NNK-induced lung tumors (Figure 1A and A-i). Likewise, tumors from the NNK+LPS group showed significantly higher number of macrophages than SNLT (Figure 1B and B-i). On the other hand, the abundance of TANs was not different either between NNK-induced and NNK+LPS-induced lung tumors or NNK+LPS-induced lung tumor tissue and SNLT. Because TAMs from established tumors are generally skewed toward the anti-inflammatory, immunosuppressive and protumorigenic M2 phenotype (26), we determined the abundance of M2 TAMs ($CD45^+F4/80^+CD206^+$) in NNK+LPS-induced lung tumors. As shown in Figure 1C, 45% of macrophages in NNK+LPS-induced lung tumors were $CD206^+$, a marker for M2 macrophages. In line with the higher abundance of M2 macrophages in the NNK+LPS group, the expression of arginase I, a marker for M2 macrophages, was significantly higher in the NNK+LPS group than in the NNK and negative control groups (Supplementary Figure 2, available at *Carcinogenesis* Online). However, the expression of indoleamine 2,3-dioxygenase, the rate-limiting tryptophan-degrading enzyme produced by macrophages and dendritic cells and acts as an important T cell immunomodulator and inducer of tolerance, and interleukin (IL)-10, a potent activator of indoleamine 2,3-dioxygenase, was lower in the NNK and NNK+LPS groups compared with the level in the vehicle group (Supplementary Figure 2, available at *Carcinogenesis* Online). These findings are in line with the report that indoleamine 2,3-dioxygenase activity was progressively reduced in patients with COPD of increasing clinical severity and resulted in the induction of IL-17A and concomitant loss of IL-10 secretion (27). TAMs are also known to express higher levels of PD-1 and PD-L1, and overexpression of PD-1 and PD-L1 in macrophages has been associated with reduced phagocytosis (28) and inactivation of CD8 T cells (29), respectively. In our studies, $PD\text{-}1^+$ TAMs were found to be significantly more abundant in NNK+LPS-induced lung tumors (23%) compared with NNK-induced lung tumors (6%, Figure 1D and D-i). On the other hand, the abundance of

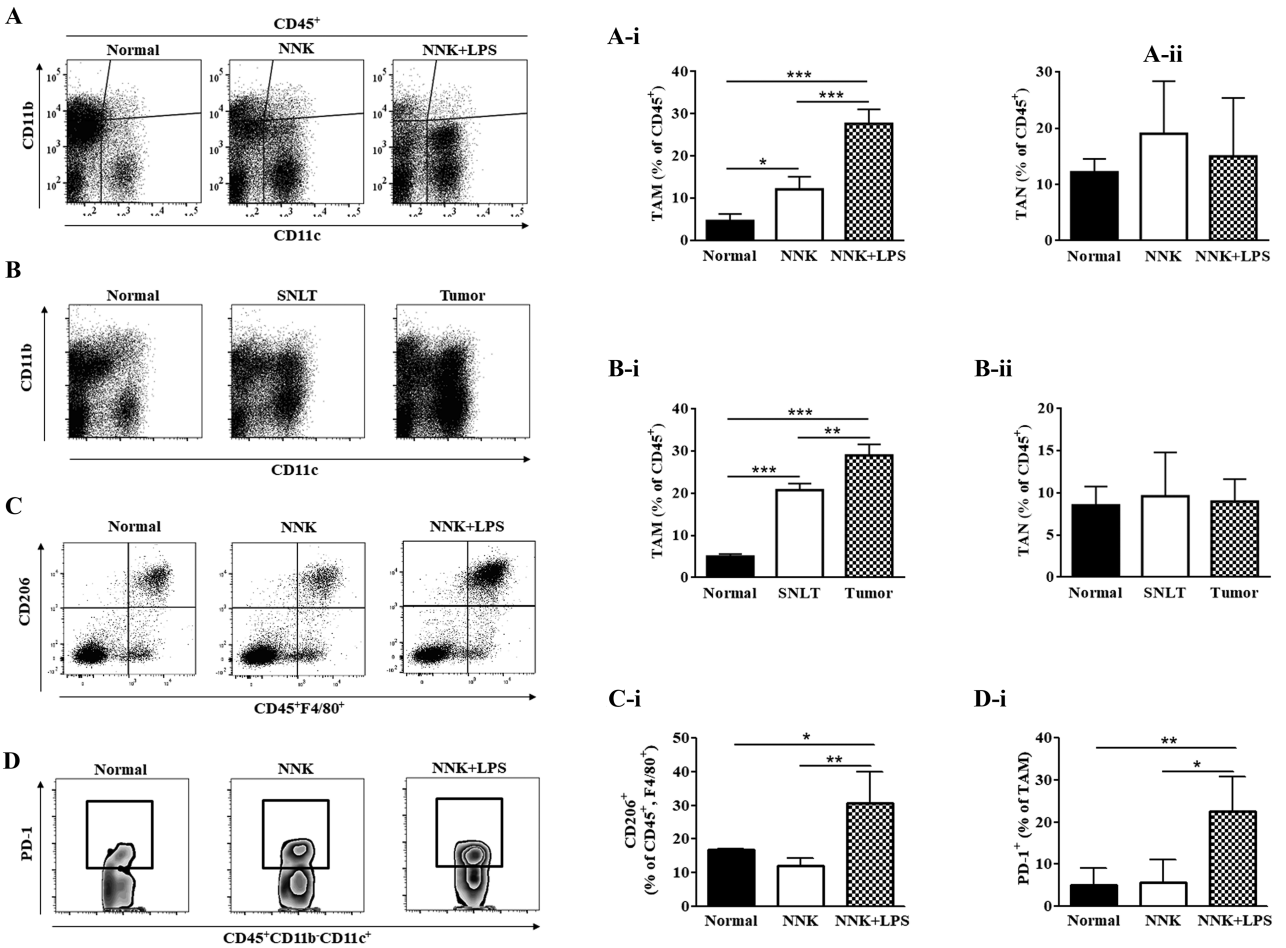

Figure 1. Differential infiltration of NNK- and NNK+LPS-induced lung tumors by macrophages. (**A** and **B**) Representative flow cytometry plots showing the relative abundance of TAMs ($CD45^+$ $CD11b^-$ $CD11c^+$) and TANs ($CD45^+$ $CD11b^+$ $Ly6G^+$) in NNK+LPS-induced lung tumors, NNK-induced lung tumors and normal lung tissue from vehicle-treated mice (A) or NNK+LPS-induced lung tumors, SNLT of these tumors and normal lung tissues from the vehicle group (B). Quantification of TAMs (**A-i** and **B-i**) and TANs (**A-ii** and **B-ii**) in the different lung tissues as determined by flow cytometry (mean ± SEM, $P < 0.05$). (**C** and **D**) Abundance of M2 TAMs ($CD45^+$ $F4/80^+$ $CD206^+$; C) and PD-1^+ TAMs ($CD45^+$ $CD11b^-$ $CD11c^+$ $Ly6G^+$ PD-1^+, D, D-i) in the different groups of mice. Flow cytometry analysis was carried out at least three times and each time two mice (vehicle group) or two to three mice (NNK- or NNK+LPS-treated mice) were used.

PD-$L1^+$ TAMs was low in both groups, and no difference was observed between NNK- and NNK+LPS-induced lung tumors (data not shown).

T lymphocyte infiltration into NNK- and NNK+LPS-induced lung tumors

To determine the abundance and phenotype of T cells within NNK- and NNK+LPS-induced mouse lung tumors, we analyzed the percentage of $CD3^+$, $CD8^+$ and $CD4^+$, $Foxp3^+$ and PD-1^+ T lymphocytes by flow cytometry. The infiltration rate of total $CD3^+$ T lymphocytes as well as the subsets $CD8^+$ and $CD4^+$ lymphocytes in NNK+LPS-induced lung tumors was similar to that observed in NNK-induced lung tumors (Figure 2A and Ai-iii). However, the expression of Granzyme B, the product of cytotoxic $CD8^+$ T cells, was significantly lower in NNK- and NNK+LPS-induced lung tumors compared with the expression in the negative control group, whereas IL-17, a proinflammatory cytokine produced by T cells, was significantly higher in the NNK+LPS group than in the NNK or negative control group (Supplementary Figure 3, available at *Carcinogenesis* Online). Further analyses of $CD8^+$ and $CD4^+$ lymphocytes showed that both groups of lymphocytes were more abundant in the tumor tissue than in the SNLT although the differences were not statistically significant (data not shown). Separation of $CD8^+$ and $CD4^+$ lymphocytes into $Foxp3^+$ and $Foxp3^-$ T lymphocytes indicated that infiltration of $CD4^+$ $Foxp3^+$ and $CD8^+$ $Foxp3^+$ cells was higher in NNK+LPS-induced lung tumors (21 and 24%, respectively, Figure 2B, Bi and Bii) than in the NNK group (11 and 13%, respectively). Similarly, the proportions of $CD4^+$ PD-1^+ and $CD8^+$ PD-1^+ T lymphocytes were significantly higher in lung tumors from the NNK+LPS group as compared with the level in tumors induced by NNK (53 versus 20% for $CD4^+$ PD-1^+ lymphocytes and 44 versus 19% for $CD8^+$ PD-1^+ T lymphocytes, Figure 2C, C-i and C-ii). In fact, the abundance of these subsets of lymphocytes in NNK-induced lung tumors was similar to that observed in normal mouse lung tissue.

Differential expression of PD-L1 in NNK+LPS-induced lung tumors in mice

To determine the relative expression of PD-L1 in lung tumor cells from NNK- and NNK+LPS-treated mice as well as normal lung cells from the vehicle-treated mice, $CD45^-$ $CD31^-$ $EPCAM^+$ cells (cells negative for markers of immune and endothelial cells but positive for epithelial cell marker) were separated and further

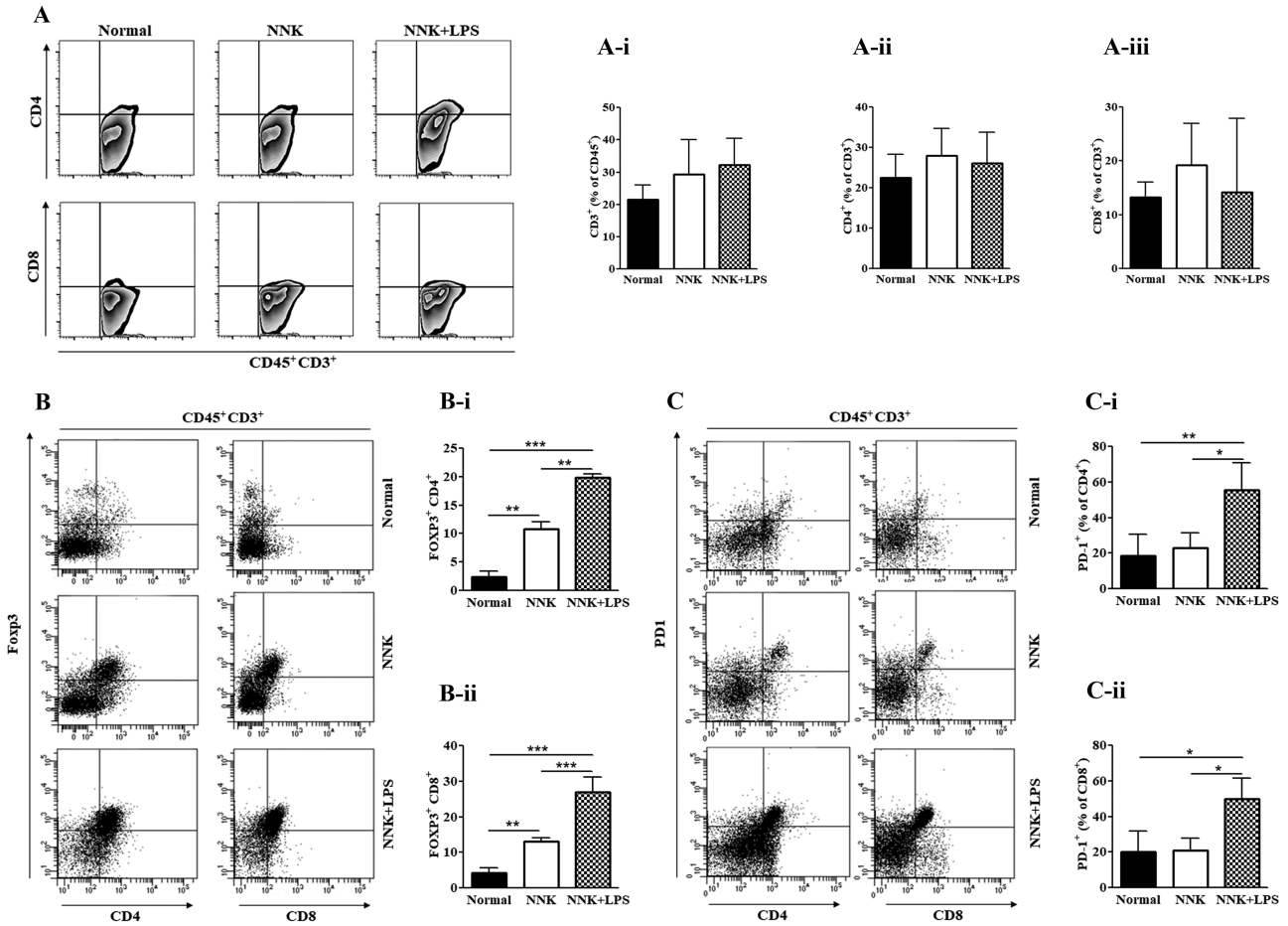

Figure 2. Infiltration of lung tumors by T lymphocytes. (**A–C**) Representative flow cytometry plots for $CD3^+$, $CD4^+$ and $CD8^+$ T cells (A), $FOXP3^+$ T cells (B), and $CD4^+$ $PD\text{-}1^+$ and $CD8^+$ $PD\text{-}1^+$ (C) T cells within lung tissues of the different groups of mice. (**A-i–C-ii**) Quantification of $CD3^+$, $CD4^+$ and $CD8^+$ T cells (Ai, Aii and A-iii, respectively), $FOXP3^+$ $CD4^+$ (B-i), $FOXP3^+$ $CD8^+$ (B-ii), $PD\text{-}1^+$ $CD4^+$ (C-i) and $PD\text{-}1^+$ $CD8^+$ (C-ii) T cells within lung tissues of the different groups of mice. Flow cytometry analysis was carried out at least three times and each time two mice (vehicle group) or two to three mice (NNK- or NNK+LPS-treated mice) were used. Data represent mean ± SEM; $P < 0.05$.

interrogated for PD-L1 expression. As depicted in Figure 3A and A-i, the abundance of $PD\text{-}L1^+$ lung tumor cells was significantly higher (43%) in the NNK+LPS group compared with lung tumor cells from the NNK group (23%) in which the abundance of these cells was similar to the level observed in normal lung tissues from vehicle-treated mice. $CD44^+$ tumor-initiating cells have been shown to selectively evade the host immune response by overexpressing PD-L1 (30). In line with this report, interrogation of $CD45^-$ $CD31^-$ $EPCAM^+$ $PD\text{-}L1^+$ cells for the expression of CD44 showed that, in the NNK+LPS group, ~56% of $PD\text{-}L1^+$ tumor cells were $CD44^+$, which as more than 2-fold higher than the level observed in NNK-induced lung tumors or normal lungs (Figure 3B and B-i).

Modulation of PD-1/PD-L1 expression in THP-1 cells treated with LPS or grown in CM generated by NSCLC cells

To determine whether inflammatory agents or the crosstalk between lung cancer cells and macrophages enhance the expression of PD-1/PD-L1 in macrophages under *in vitro* condition, PMA-activated THP-1 cells, which differentiated into macrophages, were treated with different concentrations of LPS or grown in CM prepared from NSCLC cells and changes in the level of PD-1 and PD-L1 were analyzed by qRT–PCR, Western immunoblotting and flow cytometry. As depicted in Figure 4A, whereas high concentration of LPS (10 μg/ml) was required to induce PD-1, PD-L1 was significantly regulated by a 10-fold lower concentration of LPS (1 μg/ml). Likewise, LPS induced a marked increase in the protein abundance of PD-L1 (Figure 4B and C), but not PD-1 (data not shown). Next, we assessed if macrophages grown in CM generated by A549, H838 and H1650 NSCLC cells exhibit modulations in the level of PD-1 and PD-L1. CM from all three NSCLC cells increased the expression of PD-L1 (Figure 4D and E), but not PD-1 (data not shown) in macrophages, suggesting that the crosstalk between NSCLC cells and macrophages increases the abundance of PD-L1 in the latter cells. It has been recently shown that mammary cancer cells regulate PD-L1 expression in tumor-associated macrophages via COX2/mPGES1/PGE2 pathway (31). However, although our studies in macrophages grown in CM generated by A549, H838 and H1650 NSCLC cells exhibited a strong increase in the expression of COX-2 (Figure 4F) and COX-2-specific siRNAs consistently abolished COX-2 expression, the effects on PD-L1 were unclear (Figure 4G).

CM generated by macrophages induced PD-L1 expression in NSCLC cells and this effect was attenuated by EGFR and ERK inhibitors

To determine whether the expression of PD-L1 in NSCLC cells is modulated as a result of the crosstalk between NSCLC cells

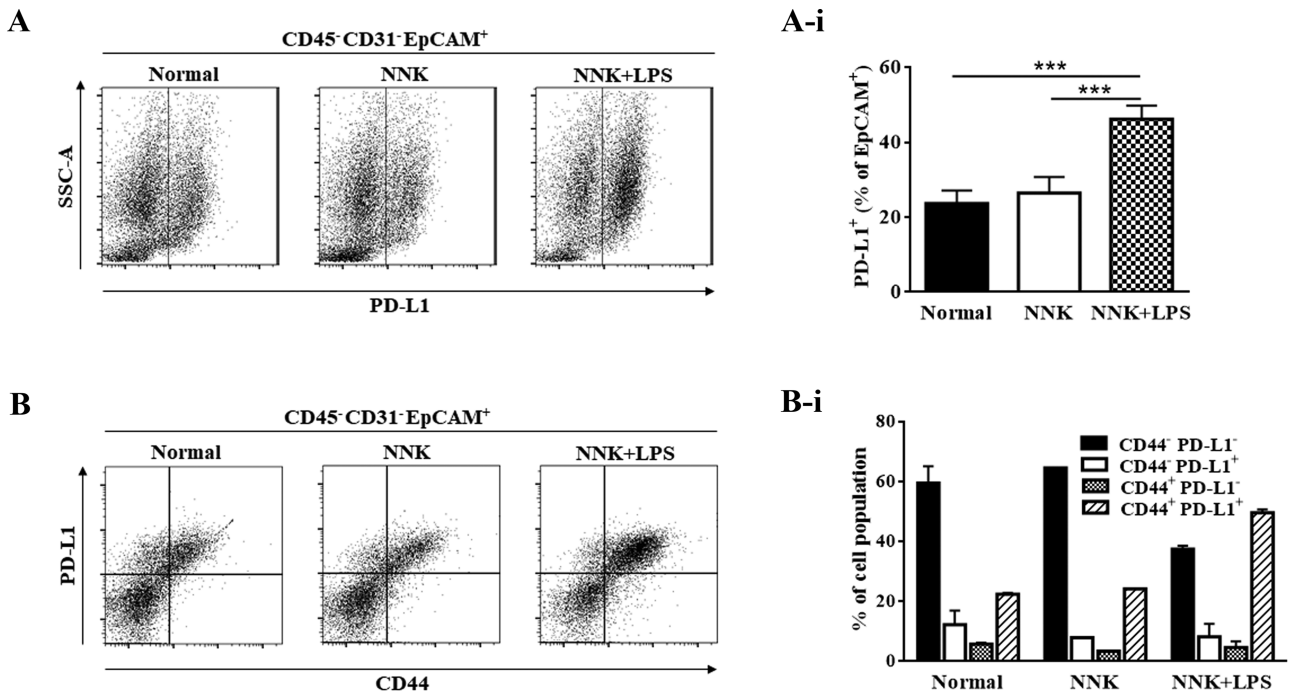

Figure 3. Differential expression of PD-L1 by NNK- and NNK+LPS-induced lung tumors. (**A** and **B**) Representative flow cytometry plot for CD45⁻ CD31⁻ EPCAM⁺ PD-L1⁺ (A) and CD45⁻ CD31⁻ EPCAM⁺ PD-L1⁺ CD44⁺ (B) lung cells in lung tissues of the different groups of mice. (A-i and B-i) Quantification of CD45⁻ CD31⁻ EPCAM⁺ PD-L1⁺ (A-i) and CD45⁻ CD31⁻ EPCAM⁺ PD-L1⁺ CD44⁺ (B-i) lung cells by flow cytometry within normal lung tissues from vehicle-treated mice and NNK- or NNK+LPS-induced lung tumors. Flow cytometry analysis was carried out with two mice for the vehicle group and three mice each for the NNK and NNK+LPS groups with the exception of B-i results in which the NNK data were collected only from one mouse. Data represent mean ± SEM; $P < 0.05$.

and macrophages, NSCLC cells were incubated in CM generated by macrophages and modulation of PD-L1 mRNA and protein levels were assessed. As shown in Figure 5A–D, CM generated by macrophages significantly increased not only the mRNA expression of PD-L1 (Figure 5A), but also the abundance of PD-L1 protein (Figure 5B and C). Furthermore, we observed that MG132, a specific inhibitor of the 26S proteasome, elevated PD-L1 accumulation in H1975 cells, although the effects were not clearly dose dependent (Figure 5D), suggesting that PD-L1 is regulated via a post-transcriptional regulation mechanism through degradation by the proteasomal pathway. Previous studies have shown that the expression of PD-L1 in cancer cells was regulated by several pathways, including EGFR, PI3K/Akt, MEK/ERK and JAK/STAT3 pathways (32). Attempts to assess the involvement of these pathways in macrophage CM-induced overexpression of PD-L1 in NSCLC cells showed that macrophage CM markedly increased levels of EGFR, p-EGFR, ERK, p-ERK and Akt in A549 cells, while effects in H1975 cells were unclear (Figure 5E). Upon treatment with erlotinib or U0126, inhibitors of EGFR and ERK, respectively, the levels of p-EGFR and p-ERK were clearly reduced in A549 cells grown in CM generated by macrophages, but these effects did not suppress the expression of P-D-L1 (Figure 5F). On the other hand, in 1975 cells grown with and without CM, erlotinib decreased the level of p-EGFR and PD-L1, whereas U0126 completely abrogated the expression of p-ERK and markedly reduced the level of both p-EGFR and PD-L1.

Regulation of PD-L1 expression by the IFNγ–STAT1/STAT3 axis

Various immune cells of mice overexpress IFNγ in response to LPS treatment (33) and studies in melanoma cell lines and specimens from patients with melanoma have revealed that the interferon receptor signaling pathway regulates PD-L1 expression (34). To determine whether the interferon receptor signaling pathway is involved in regulating PD-L1 expression in lung tumorigenesis, first, we determined levels of IFNγ, total and phosphorylated STAT1, total and phosphorylated STAT3, and PD-L1 in normal mouse lungs tissues from vehicle-treated mice and lung tumors from NNK- or NNK+LPS-treated mice. As depicted in Figure 6A, lung tumors from NNK+LPS-treated mice exhibited the highest expression of IFNγ, total and phosphorylated STAT1, total and phosphorylated STAT3, and PD-L1. In the next study in which A549 lung adenocarcinoma cells were exposed to IFNγ for different periods of time (1 min to 48 h) and the expression of total and phosphorylated STAT1 and PD-L1 were determined, the level of P-STAT1 was upregulated beginning 1 min after exposure to IFNγ, but the expression of total STAT1 and PD-L1 increased beginning 16 h after exposure to IFNγ (Figure 6B). Finally, to further corroborate that PD-L1 is regulated by STAT1 in A549 cells, these cells were exposed to specific siRNAs against STAT1 and modulation of PD-L1 expression was assessed. In line with the above results, we observed, despite differential efficacies among the different siRNAs, that the expression of PD-L1 was suppressed (Figure 6C).

Discussion

In the present study, we assessed the immune microenvironment of NNK-induced mouse lung tumors harboring COPD-like airway inflammation induced by repetitive doses of LPS. Moreover, we determined modulation of PD-L1 expression resulting from the interaction between macrophages and NSCLC cells and the potential mechanisms involved. We found that the abundance of CD3⁺, CD4⁺ and CD8⁺ T cells in NNK+LPS-induced lung tumors was not significantly different from the levels observed in the

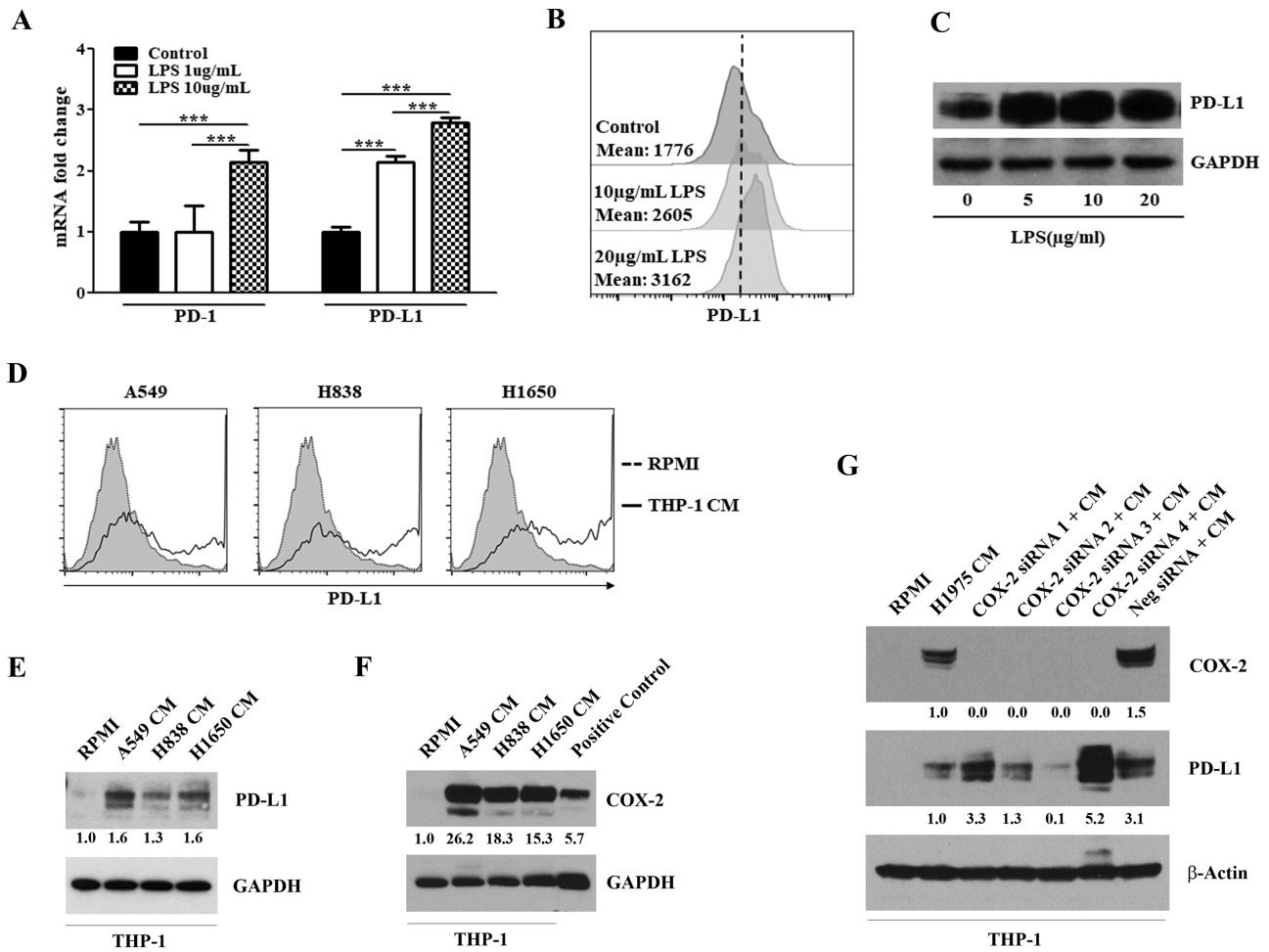

Figure 4. LPS or CM generated by NSCLC cells modulated the level of PD-1/PD-L1 expression in activated THP-1 human monocytes. (**A**) LPS treatment increased the mRNA levels of PD-1 and PD-L1 in activated THP-1 cells as determined by qRT–PCR. (**B–C**) LPS increased the protein level of PD-L1 in activated THP-1 cells as determined by flow cytometry (B) and Western immunoblotting (C). (**D–F**) Incubation of activated THP-1 cells in CM generated by NSCLC cells enhanced the level of PD-L1 (D, E) and COX-2 (F). (**G**) Silencing of COX-2 with four specific COX-2 siRNA (50 nM) failed to consistently modulate NSCLC CM-induced PD-L1 expression in activated THP-1 cells.

SNLT of NNK+LPS-induced tumors, NNK-induced lung tumors or normal lung tissues from the vehicle group. However, compared with the level in the untreated control group, IL-17, a proinflammatory T cell-derived cytokine, was increased, whereas the expression of Granzyme B, a surrogate marker for cytotoxic T cells, was reduced in NNK and NNK+LPS groups, and more so in the latter group than the former one. $CD4^+$ and $CD8^+$ T lymphocytes infiltrating NNK+LPS-induced lung tumors exhibited remarkably higher expression of FoxP3, a marker for T-regs, and PD-1, compared with $CD4^+$ and $CD8^+$ T lymphocytes isolated from NNK-induced lung tumors or normal mouse lungs. Additionally, NNK+LPS-induced lung tumors as well as the SNLT of NNK+LPS-induced tumors were highly infiltrated with macrophages which showed a strong expression of CD206, a marker for alternatively polarized protumorigenic and immunosuppressive M2 macrophages, as well as PD-1. Compared with NNK-induced lung tumor cells, a significantly higher percentage of NNK+LPS-induced lung tumor cells expressed PD-L1 and ~50% of these $PD\text{-}L1^+$ lung tumor cells co-expressed CD44, a marker for putative cancer stem cells. Overall, our findings suggest that the higher lung tumor burden in NNK+LPS-treated mice, compared with NNK-treated mice, could be ascribed, at least in part, to the highly immunosuppressive tumor microenvironment which permits enhanced proliferation and survival of lung tumor cells.

Our *in vitro* assays in which macrophages were incubated in CM generated by NSCLC cells or NSCLC cells were grown in CM produced by macrophages suggest that the crosstalk between lung cancer cells and macrophages in the tumor microenvironment increases the expression of PD-L1 in both cells.

Consistent with our findings, studies in a KRAS model of lung cancer showed that COPD-like lung inflammation induced by *Haemophilus infuenzae* (NTHi) was associated with overexpression of IL-17C, PD-1 (CD8 lymphocytes) and PD-L1 in the tumor microenvironment (35). Furthermore, tumor growth was decreased in IL-17C deficient mice, but not in wild-type mice, after anti-PD-1 treatment, suggesting that strategies targeting innate immune mechanisms, such as blocking of IL-17C, may improve the response to anti-PD-1 treatment in lung cancer patients. Assessment of the effect of NTHi-induced inflammation on neutrophil recruitment showed that neutrophils were recruited to the tumor microenvironment within 4 h after a single exposure to NTHi. Contrary to these findings, in the present study in which mice received weekly LPS treatment for 14 weeks and killed at week 30, LPS-induced inflammation increased the accumulation of macrophages, but not neutrophils, in the microenvironment of NNK-induced lung tumors, indicating that neutrophils are minor players in the later stages of COPD-like inflammation. In line with our findings, a study by Moghaddam *et al.* in mice

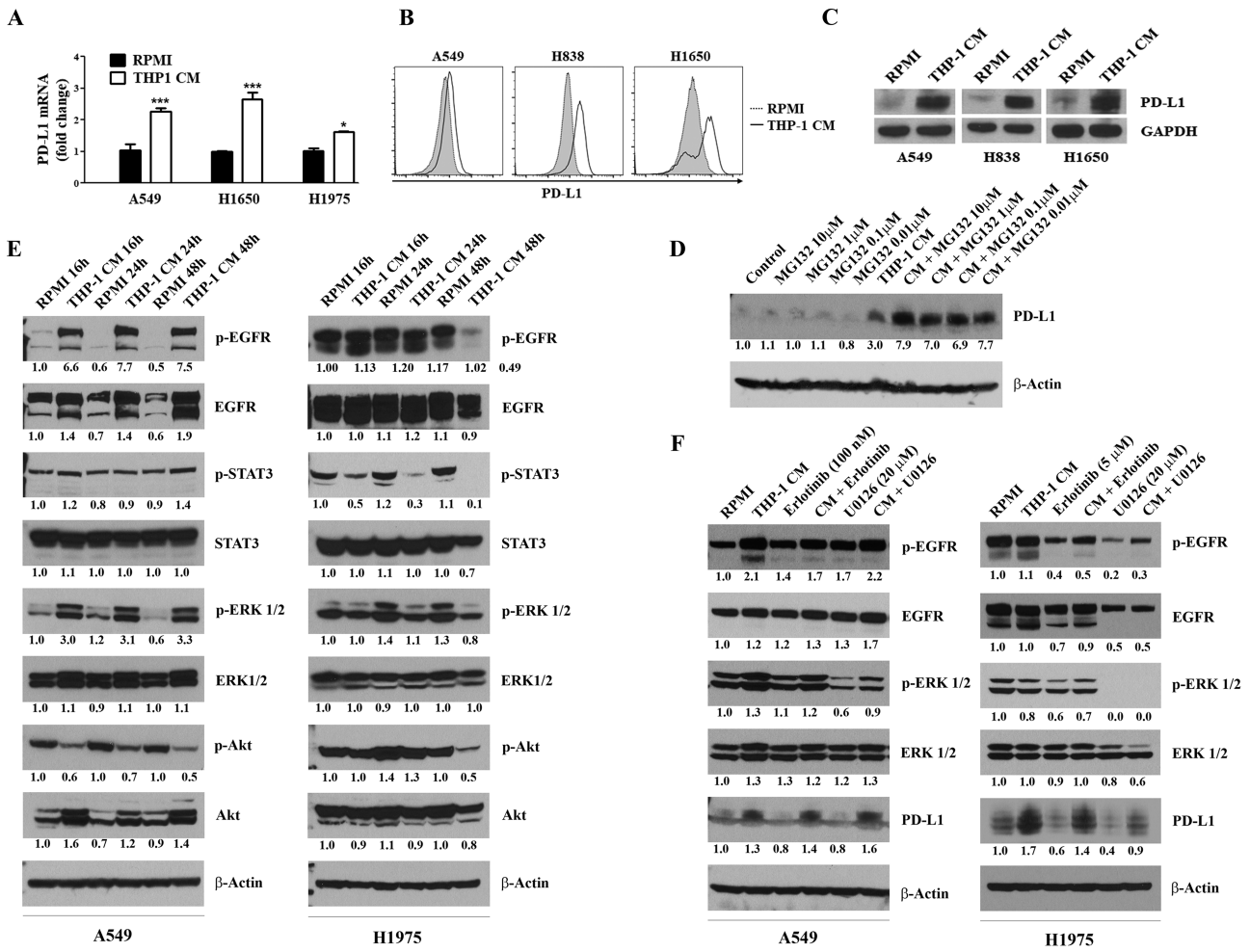

Figure 5. THP-1 CM enhanced PD-L1 expression in NSCLC cells. (**A–C**) Incubation of NSCLC cells in CM generated by activated THP-1 cells increased the mRNA (A) and protein (B, C) levels of PD-L1. NSCLC cells were incubated in normal RPMI or CM generated by macrophages for 24 h, and the mRNA (by qRT–PCR) and protein (flow cytometry and Western immunoblotting) levels of PD-L1 were determined. (**D**) Effect of MG132, a proteasome inhibitor, on PD-L1 expression in A549 cells. A549 cells grown in normal RPMI media or macrophage CM were treated with different concentrations of MG132 (0.01, 0.1 or 1 μM) for 24 h, and levels of PD-L1 were determined by Western immunoblotting. (**E**) Modulation, by macrophage CM, of cell proliferation- and survival-related signaling pathways in NSCLC cells. NSCLC cells were grown as described above, cell lysates prepared and levels of EGFR, p-EGFR, EGFR, STAT3, p-STAT3, ERK, p-ERK, Akt, P-Akt were determined by Western immunoblotting. (**F**) Effects of erlotinib, EGFR inhibitor, and U0126, ERK inhibitor, on PD-L1 expression in A549 and H1975 cells. A549 and H1975 cells were grown in normal RPMI media or CM generated by macrophages, treated with erlotinib (100 nM or 5 μM) or U0126 (20 μM) for 24 h. Subsequently, cell lysates were prepared and levels of PD-L1 were determined by Western immunoblotting. Densitometry measurements were performed to determine the relative expression of the different proteins relative to the level in cell grown in normal RPMI media and treated with dimethyl sulfoxide. Experiments were performed at least three times and representative Western blots are shown.

exposed to the aerosolized NTHi lysate showed that the number of BALF neutrophils peaked on the second day after exposure, declined markedly on the third day and returned to baseline by the seventh day, whereas the numbers of macrophages increased significantly on the second day after exposure and remained elevated several-fold on the seventh day (36). Likewise, lung tissue sections of mice repeatedly exposed to LPS for 12 weeks showed a profound accumulation of macrophages, but pulmonary infiltration of neutrophils, which was observed to occur after each LPS exposure, was absent indicating that acute inflammatory changes were resolved at this time point (37). Long-term exposure (up to 6 months) of rats to cigarette smoke also resulted in an increase in the number of lung macrophages at month 2 which continued to month 6, whereas the number of lung neutrophils increased at month 1 of smoke exposure and reduced to control levels at months 2–6 (38).

Similar to the findings in our animal model, studies in COPD patients showed a skewed M1 to M2 polarization of macrophages (39,40), increased accumulation of functionally suppressive T-regs and elevated expression of PD-1 on effector T cells (8,10). Moreover, compared with lung cancer patients without COPD, patients with lung cancer and COPD exhibited a higher infiltration of the tumor tissue by CD8 or CD4 T cells overexpressing PD-1 and T cell immunoglobulin- and mucin-domain-containing molecule-3 (TIM-3), a negative regulatory molecule of T cells (9,23). The increased response of these patients to immune checkpoint blockade therapy was attributed to the higher abundance of PD-1-expressing CD8 T cells.

One mechanism through which tumor-associated macrophages (TAMs) enhance tumorigenesis appears to be via expression of immunosuppressive checkpoint proteins (28,41–43). A high percentage of both human and mouse TAMs express surface PD-1 in contrast with circulating monocytes or splenic macrophages, which expressed no detectable level of the protein (28). In the aforementioned study, PD-1expression by TAMs was negatively correlated with phagocytic potency

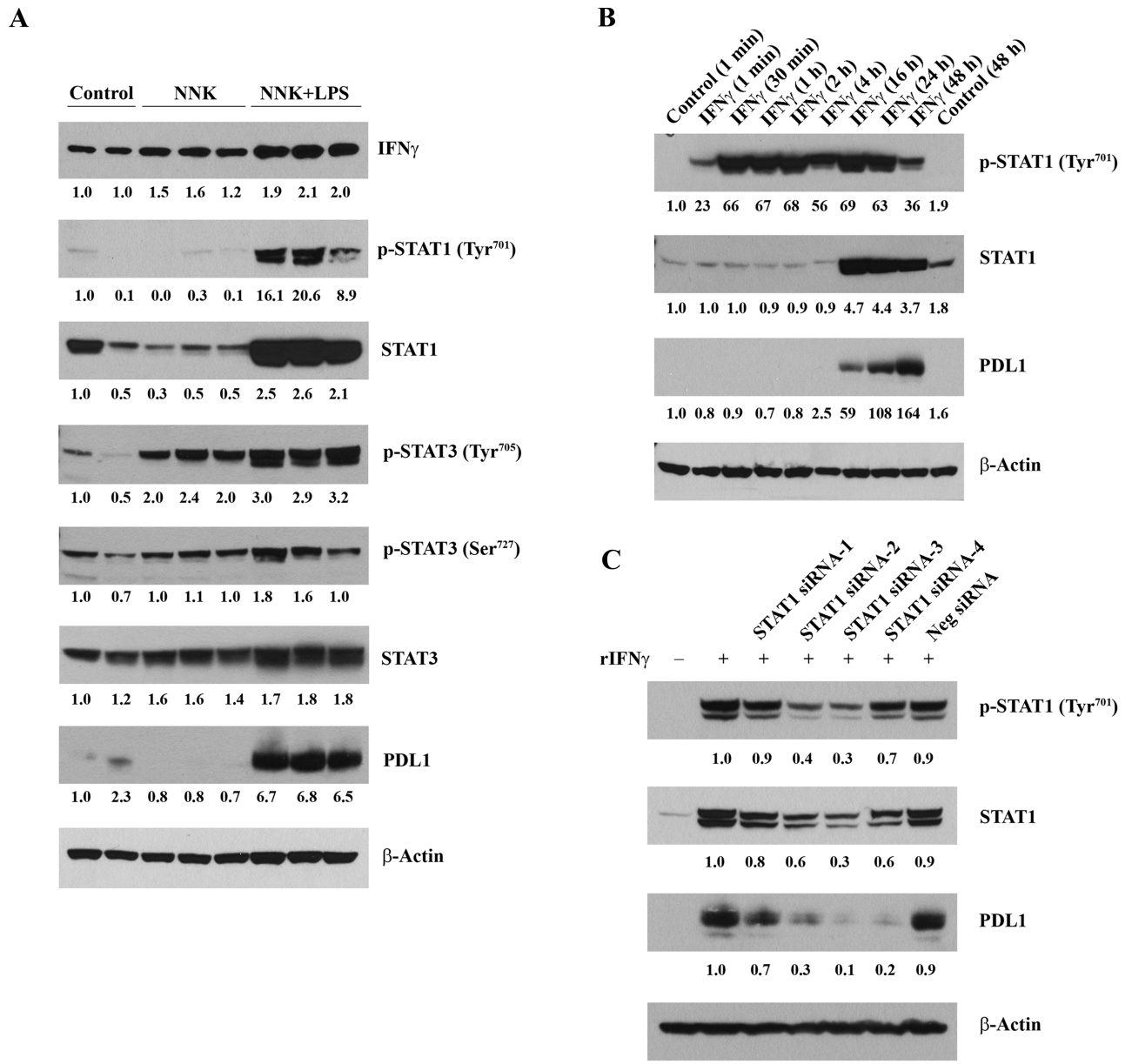

Figure 6. IFNγ-mediated regulation of PD-L1 in lung tumor cells. (**A**) Differential levels of IFNγ, total and phosphorylated STAT1, total and phosphorylated STAT3, and PD-L1. Lung tissue samples were lysed in RIPA buffer, extracted protein was denatured, 50 μg each were resolved on 4–12% gradient acrylamide gels, blotted on polyvinylidene difluoride (PVDF) membranes and developed by enhanced chemiluminescence (ECL) method. (**B**) Time-dependent induction of total and phosphorylated STAT1 and PD-L1 by IFNγ. A549 cells were treated with 10 ng/ml recombinant human IFNγ for different time intervals as indicated, lysed in RIPA buffer, 50 μg each of the extracted protein samples were resolved on 4–12% gradient acrylamide gels, blotted on PVDF membranes and developed by ECL method. (**C**) Silencing of *STAT1* by specific siRNAs suppresses PD-L1 expression in A549 cells. A549 cells were treated with four different anti-*STAT1* siRNA (Qiagen) and AllStars Negative siRNA for 48 h, followed by 1 ng/ml recombinant human IFNγ for 24 h, lysed in RIPA buffer, 50 μg each of the extracted protein samples were resolved on 4–12% gradient acrylamide gels, blotted on PVDF membranes and developed by ECL method.

against tumor cells and blockade of PD-1/PD-L1 interaction increased macrophage phagocytosis and reduced tumor burden in a macrophage-dependent fashion. In the present study, we found a higher abundance of PD-1$^+$ TAMs in NNK+LPS-induced lung tumors when compared with NNK-induced lung tumors, which could contribute to reduced phagocytic potency against lung tumor cells. Our studies on the potential regulation of PD-L1 by LPS showed that whereas macrophages treated with low concentrations of LPS under *in vitro* conditions exhibited overexpression of PD-L1, mice treated with LPS for 14 weeks failed to exhibit similar effects. This discrepancy could be associated with the status of macrophage polarization. In response to single treatment with low concentration of LPS, as in our *in vitro* studies or studies by other groups (44), macrophages undergo M1 activation, characterized by the expression and secretion of proinflammatory cytokines such as tumor necrosis factor-α, which has been shown to upregulate PD-L1 expression in murine tumor-associated monocytes and macrophages (45). On the other hand, repeated exposure to LPS, as in our *in vivo* studies, leads to tolerance and M2 polarization of macrophages (46) and M2 macrophages are predominantly PD-1 (28) and PD-L2$^+$ (47). Moreover, our results in the *in vivo* model are in line with previous reports in which the expression of PD-L1 by lung macrophages and dendritic cells

was found to be compromised in COPD patients (48), which suggests that despite the efficacy of PD-1 inhibitors in NSCLC patients, further inhibition of the impaired PD-1–PD-L1 axis in COPD could increase airway inflammation and thus promote disease progression.

Although a high number of human or mouse tumor cell lines do not constitutively express PD-L1, most tumors express elevated levels of PD-L1, suggesting that PD-L1 can be induced in tumor cells via a crosstalk between tumor cells and other cells in the tumor microenvironment (44,49,50). In line with this, in the present study, CM generated by macrophages induced PD-L1 in NSCLC cells devoid of constitutive PD-L1 expression and markedly increased PD-L1 in NSCLC cells which express the protein constitutively. Further studies on signaling pathways involved in these effects revealed that inhibition of EGFR and ERK negatively regulated PD-L1 expression in EGFR mutant 1975 cells, but not in EGFR wild-type A549 cells, implying that EGFR-TKIs/ERK inhibitors may potentiate the efficacy of PD-1/PD-L1 immune checkpoint blockade in lung cancer patients but the type of genetic alterations may influence these responses. The interferon receptor signaling axis (IFNγ–JAK/SAT1/STAT3) and COX-2/PGE2 signaling pathways have also been shown to regulate PD-L1 expression in pancreatic carcinoma and tumor-infiltrating-myeloid cells (31), respectively. In our study, levels of IFNγ, STAT1/STAT3 and PD-L1 were overexpressed in lung tumor tissues of mice treated with NNK+LPS and A549 cells exhibited overexpression of STAT1 and PD-L1 in response to IFNγ treatment. Silencing of STAT1 with specific siRNAs in A549 cells, suppressed the expression of PD-L1. Together, these results indicate the importance of the interferon receptor signaling pathway in regulating PD-L1 expression in lung tumors. On the other hand, although macrophages cultured in CM generated by H1975 NSCLC cells exhibited a strong increase in COX-2 expression, downregulation of COX-2 by specific siRNAs failed to clearly reduce levels of PD-L1, suggesting that COX-2/PGE2 pathway does not regulate PD-L1 expression in these cells.

In conclusion, our results showed that LPS-induced COPD-like chronic inflammation enhances not only PD-L1 expression in lung tumor cells but also the infiltration of lung tumors with type 2-polarized TAMs, PD-1$^+$ TAMs, T-regs, and PD-1$^+$ CD4 and CD8 T cells. This immunosuppressive environment could be responsible for the higher tumor burden in NNK+LPS-treated mice when compared with mice treated with NNK only. However, this immunosuppressive environment might also increase the response of NNK+LPS-induced lung tumors to immune checkpoint blockade as has been reported in lung cancer patients harboring COPD (9,23,24).

Supplementary material

Supplementary data are available at *Carcinogenesis* online.

Funding

This study was financially supported by National Institutes of Health/National Cancer Institute grant (RO1CA166615-01 to F.K.).
Conflict of Interest Statement: No potential conflicts of interest were disclosed by all authors.

References

1. Siegel, R.L. *et al.* (2019) Cancer statistics, 2019. *CA Cancer J. Clin.*, 69, 7–34.
2. de Torres, J.P. *et al.* (2011) Lung cancer in patients with chronic obstructive pulmonary disease – incidence and predicting factors. *Am. J. Respir. Crit. Care Med.*, 184, 913–919.
3. Skillrud, D.M. *et al.* (1986) Higher risk of lung cancer in chronic obstructive pulmonary disease. A prospective, matched, controlled study. *Ann. Intern. Med.*, 105, 503–507.
4. Young, R.P. *et al.* (2009) COPD prevalence is increased in lung cancer, independent of age, sex and smoking history. *Eur. Respir. J.*, 34, 380–386.
5. Durham, A.L. *et al.* (2015) The relationship between COPD and lung cancer. *Lung Cancer*, 90, 121–127.
6. Masri, F.A. *et al.* (2005) Abnormalities in nitric oxide and its derivatives in lung cancer. *Am. J. Respir. Crit. Care Med.*, 172, 597–605.
7. Pignatelli, B. *et al.* (2001) Nitrated and oxidized plasma proteins in smokers and lung cancer patients. *Cancer Res.*, 61, 778–784.
8. Bhat, T.A. *et al.* (2015) Immune dysfunction in patients with chronic obstructive pulmonary disease. *Ann. Am. Thorac. Soc.*, 12(Suppl 2), S169–S175.
9. Biton, J. *et al.* (2018) Impaired tumor-infiltrating T cells in patients with chronic obstructive pulmonary disease impact lung cancer response to PD-1 blockade. *Am. J. Respir. Crit. Care Med.*, 198, 928–940.
10. Kalathil, S.G. *et al.* (2014) T-regulatory cells and programmed death 1+ T cells contribute to effector T-cell dysfunction in patients with chronic obstructive pulmonary disease. *Am. J. Respir. Crit. Care Med.*, 190, 40–50.
11. Agata, Y. *et al.* (1996) Expression of the PD-1 antigen on the surface of stimulated mouse T and B lymphocytes. *Int. Immunol.*, 8, 765–772.
12. Liang, S.C. *et al.* (2003) Regulation of PD-1, PD-L1, and PD-L2 expression during normal and autoimmune responses. *Eur. J. Immunol.*, 33, 2706–2716.
13. Stanciu, L.A. *et al.* (2006) Expression of programmed death-1 ligand (PD-L) 1, PD-L2, B7-H3, and inducible costimulator ligand on human respiratory tract epithelial cells and regulation by respiratory syncytial virus and type 1 and 2 cytokines. *J. Infect. Dis.*, 193, 404–412.
14. Zdrenghea, M.T. *et al.* (2012) Role of PD-L1/PD-1 in the immune response to respiratory viral infections. *Microbes Infect.*, 14, 495–499.
15. Brahmer, J. *et al.* (2015) Nivolumab versus docetaxel in advanced squamous-cell non-small-cell lung cancer. *N. Engl. J. Med.*, 373, 123–135.
16. Chen, Y.B. *et al.* (2012) Clinical significance of programmed death-1 ligand-1 expression in patients with non-small cell lung cancer: a 5-year-follow-up study. *Tumori*, 98, 751–755.
17. Pardoll, D.M. (2012) The blockade of immune checkpoints in cancer immunotherapy. *Nat. Rev. Cancer*, 12, 252–264.
18. Velcheti, V. *et al.* (2014) Programmed death ligand-1 expression in non-small cell lung cancer. *Lab. Invest.*, 94, 107–116.
19. Gettinger, S.N. *et al.* (2015) Overall survival and long-term safety of nivolumab (anti-programmed death 1 antibody, BMS-936558, ONO-4538) in patients with previously treated advanced non-small-cell lung cancer. *J. Clin. Oncol.*, 33, 2004–2012.
20. Herbst, R.S. *et al.* (2014) Predictive correlates of response to the anti-PD-L1 antibody MPDL3280A in cancer patients. *Nature*, 515, 563–567.
21. Reck, M. *et al.*; KEYNOTE-024 Investigators. (2016) Pembrolizumab versus chemotherapy for PD-L1-positive non-small-cell lung cancer. *N. Engl. J. Med.*, 375, 1823–1833.
22. Rizvi, N.A. *et al.* (2015) Activity and safety of nivolumab, an anti-PD-1 immune checkpoint inhibitor, for patients with advanced, refractory squamous non-small-cell lung cancer (CheckMate 063): a phase 2, single-arm trial. *Lancet. Oncol.*, 16, 257–265.
23. Mark, N.M. *et al.* (2018) Chronic obstructive pulmonary disease alters immune cell composition and immune checkpoint inhibitor efficacy in non-small cell lung cancer. *Am. J. Respir. Crit. Care Med.*, 197, 325–336.
24. Shin, S.H., *et al.* (2019) Improved treatment outcome of pembrolizumab in patients with nonsmall cell lung cancer and chronic obstructive pulmonary disease. *Int. J. Cancer*, 145, 2433–2439.
25. Melkamu, T. *et al.* (2013) Lipopolysaccharide enhances mouse lung tumorigenesis: a model for inflammation-driven lung cancer. *Vet. Pathol.*, 50, 895–902.
26. Conway, E.M. *et al.* (2016) Macrophages, Inflammation, and Lung Cancer. *Am. J. Respir. Crit. Care Med.*, 193, 116–130.
27. Maneechotesuwan, K. *et al.* (2013) Decreased indoleamine 2,3-dioxygenase activity and IL-10/IL-17A ratio in patients with COPD. *Thorax*, 68, 330–337.
28. Gordon, S.R. *et al.* (2017) PD-1 expression by tumour-associated macrophages inhibits phagocytosis and tumour immunity. *Nature*, 545, 495–499.

29. Hartley, G.P. *et al.* (2018) Programmed cell death ligand 1 (PD-L1) signaling regulates macrophage proliferation and activation. *Cancer Immunol. Res.*, 6, 1260–1273.
30. Lee, Y. *et al.* (2016) CD44+ cells in head and neck squamous cell carcinoma suppress T-cell-mediated immunity by selective constitutive and inducible expression of PD-L1. *Clin. Cancer Res.*, 22, 3571–3581.
31. Prima, V. *et al.* (2017) COX2/mPGES1/PGE2 pathway regulates PD-L1 expression in tumor-associated macrophages and myeloid-derived suppressor cells. *Proc. Natl Acad. Sci. USA*, 114, 1117–1122.
32. Shi, Y. (2018) Regulatory mechanisms of PD-L1 expression in cancer cells. *Cancer Immunol. Immunother.*, 67, 1481–1489.
33. Varma, T.K. *et al.* (2002) Endotoxin-induced gamma interferon production: contributing cell types and key regulatory factors. *Clin. Diagn. Lab. Immunol.*, 9, 530–543.
34. Garcia-Diaz, A. *et al.* (2017) Interferon receptor signaling pathways regulating PD-L1 and PD-L2 expression. *Cell Rep.*, 19, 1189–1201.
35. Ritzmann, F. *et al.* (2019) IL-17C-mediated innate inflammation decreases the response to PD-1 blockade in a model of Kras-driven lung cancer. *Sci. Rep.*, 9, 10353.
36. Moghaddam, S.J. *et al.* (2008) Haemophilus influenzae lysate induces aspects of the chronic obstructive pulmonary disease phenotype. *Am. J. Respir. Cell Mol. Biol.*, 38, 629–638.
37. Vernooy, J.H. *et al.* (2002) Long-term intratracheal lipopolysaccharide exposure in mice results in chronic lung inflammation and persistent pathology. *Am. J. Respir. Cell Mol. Biol.*, 26, 152–159.
38. Ofulue, A.F. *et al.* (1998) Time course of neutrophil and macrophage elastinolytic activities in cigarette smoke-induced emphysema. *Am. J. Physiol.*, 275, L1134–L1144.
39. Kaku, Y. *et al.* (2014) Overexpression of CD163, CD204 and CD206 on alveolar macrophages in the lungs of patients with severe chronic obstructive pulmonary disease. *PLoS One*, 9, e87400.
40. Vlahos, R. *et al.* (2014) Role of alveolar macrophages in chronic obstructive pulmonary disease. *Front. Immunol.*, 5, 435.
41. Kleinovink, J.W. *et al.* (2017) PD-L1 expression on malignant cells is no prerequisite for checkpoint therapy. *Oncoimmunology*, 6, e1294299.
42. Lau, J. *et al.* (2017) Tumour and host cell PD-L1 is required to mediate suppression of anti-tumour immunity in mice. *Nat. Commun.*, 8, 14572.
43. Noguchi, T. *et al.* (2017) Temporally distinct PD-L1 expression by tumor and host cells contributes to immune escape. *Cancer Immunol. Res.*, 5, 106–117.
44. Lim, S.O. *et al.* (2016) Deubiquitination and stabilization of PD-L1 by CSN5. *Cancer Cell*, 30, 925–939.
45. Hartley, G. *et al.* (2017) Regulation of PD-L1 expression on murine tumor-associated monocytes and macrophages by locally produced TNF-α. *Cancer Immunol. Immunother.*, 66, 523–535.
46. Porta, C. *et al.* (2009) Tolerance and M2 (alternative) macrophage polarization are related processes orchestrated by p50 nuclear factor kappaB. *Proc. Natl Acad. Sci. USA*, 106, 14978–14983.
47. Muraille, E. *et al.* (2014) TH1/TH2 paradigm extended: macrophage polarization as an unappreciated pathogen-driven escape mechanism? *Front. Immunol.*, 5, 603.
48. Stoll, P. *et al.* (2015) Imbalance of dendritic cell co-stimulation in COPD. *Respir. Res.*, 16, 19.
49. Zhang, Y. *et al.* (2017) Myeloid cells are required for PD-1/PD-L1 checkpoint activation and the establishment of an immunosuppressive environment in pancreatic cancer. *Gut*, 66, 124–136.
50. Jiang, X. *et al.* (2019) Role of the tumor microenvironment in PD-L1/PD-1-mediated tumor immune escape. *Mol. Cancer*, 18, 10.